Heliyon 10 (2024) e33030

Contents lists available at ScienceDirect

Heliyon

journal homepage: www.cell.com/heliyon

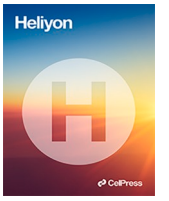

Research article

Identification of TNFAIP6 as a reliable prognostic indicator of low-grade glioma

Qinhong Huang [1], Hui Liang [1], Shenbao Shi, Yiquan Ke [**], Jihui Wang [*]

The National Key Clinical Specialty, The Engineering Technology Research Center of Education Ministry of China, Guangdong Provincial Key Laboratory on Brain Function Repair and Regeneration, Department of Neurosurgery, Zhujiang Hospital, Southern Medical University, Guangzhou, China

ARTICLE INFO

Keywords:
Low-grade glioma
Glioma stem cell-related genes
Machine learning
TNFAIP6
Glioma immune microenvironment

ABSTRACT

Glioma is the most common primary malignant tumor in the brain, characterizing by high disability rate and high recurrence rate. Although low-grade glioma (LGG) has a relative benign biological behavior, the prognosis of LGG patients still varies greatly. Glioma stem cells (GSCs) are considered as the chief offenders of glioma cell proliferation, invasion and resistance to therapies. Our study screened a series of glioma stem cell-related genes (GSCRG) based on mDNAsi and WCGNA, and finally established a reliable single-gene prognostic model through 101 combinations of 10 machine learning methods. Our result suggested that the expression level of TNFAIP6 is negatively correlated with the prognosis of LGG patients, which may be the result of pro-cancer signaling pathways activation and immunosuppression. In general, this study revealed that TNFAIP6 is a robust and valuable prognostic factor in LGG, and may be a new target for LGG treatment.

1. Introduction

Gliomas, derived from neuroepithelial cells, are the most common malignant tumor of the central nervous system. They can be classified into four grades, and grade II and III gliomas were generally defined as LGG [1,2]. The incidence rate of LGG accounts for 20–30 % in adult with the median survival time of 5.6–13.3 years, which depends on the growth rate of the tumor, histopathological characteristics and the molecular phenotype [3–6]. Although significant progress has been made in recent years in the glioma, the long-term survival rate is still poor [7–9]. Therefore, it is urgent to probe out more meaningful prognostic monitoring indicators and determine novel effective treatment strategies for glioma.

Cancer stem cells, namely a kind of cells with high reproductive potential and self-renewal ability in cancer, have been discovered in various cancers and highly express embryonic or tissue stem cell genes [10]. The cancer stem cells play an important role in tumors genesis, development, invasion, metastasis, recurrence and drug resistance [11–13]. GSCs also have the same general characteristics as mention above, and they characteristically express a series of stem cells-related markers, such as CD133, CD44, and so on; among which CD133 is one of the most reliable markers [14–17]. Studies have found that GSCs have strong resistibility to exogenous DNA damage, and can reconstruct tumors microenvironment after treatment, therefore leading to therapy resistance and tumor recurrence

* Corresponding author.
** Corresponding author.
E-mail addresses: kyquan@smu.edu.cn (Y. Ke), 346wangjihui@163.com (J. Wang).
[1] First author: Qinhong Huang& Hui Liang.

https://doi.org/10.1016/j.heliyon.2024.e33030
Received 22 April 2024; Received in revised form 12 June 2024; Accepted 13 June 2024
Available online 13 June 2024

[18,19].

Stem cell index (si) was firstly be proposed by Malta et al. and has been widely used to assess the similarity between cancer cells and stem cells [20]. According to Malta et al.'s study, the mDNAsi score can more accurately reflect the stem cell levels in glioma samples [20], and therefore, it was chosen as the key evaluation index of glioma stemness in this study.

This research identified a set of GSCRGs by evaluating the mDNAsi of each LGG samples and conducting WCGNA analysis. Finally, TNFAIP6 was identified as the most valuable prognostic GSCRG and a robust prognostic model was established. The results of immunohistochemistry further verified the accuracy of the results.

2. Materials and methods

2.1. Data sources

The DNA methylation data, RNA sequencing data and corresponding clinical information of 477 LGG patients were obtained from the Cancer Genome Atlas (TCGA, https://portal.gdc.cancer.gov). The RNA sequencing data and corresponding clinical information of 3 validation cohorts were obtained from Chinese Glioma Genome Atlas (CGGA, http://www.cgga.org.cn/). Specifically, 431 LGG samples (CGGA-1) from CGGA mRNAseq-693 dataset, 172 LGG samples (CGGA-2) from CGGA mRNAseq-325 dataset, 170 LGG samples (CGGA-3) from CGGA mRNA-array-301 dataset. The TPM data from TCGA was transform to log 2 (TPM+1) for susquent analysis.

2.2. Evaluation of glioma cell stemness

The mDNAsi score was calculated base on the DNA methylation data of each sample and standardized according to Malta et al.'s study [20]. The higher stemness level the samples have, the higher mDNAsi they score. According to the median of mDNAsi score, the selected LGG samples were grouped into high- and low-stem cell index groups, and their overall survival were analyzed.

2.3. Identification of GSCRGs

WGCNA is executed using the "WGCNA" R package. Genes that are highly correlated were classified into the same module. The module that had the strongest correlation with the sample trait was defined as interested module for subsequent analysis. Genes in interested module that are strongly corrlated with the mDNAsi were finally identified by setting the threshold of gene significance (GS) value > 0.5 as well as module membership (MM) value > 0.8 [21].

2.4. Machine learning algorithms establish prognosis-related GSCRGs

In order to establish reliable predictive features, 101 different models were developed based on 10 excellent machine learning algorithms, including "Lasso, generalized boosted modeling regression (GBM), survival support vector machine (survival-SVM), elastic network (Enet), ridge, stepwise Cox, CoxBoost. Partial least squares regression for Cox (plsRcox), random survival forest (RSF) and supervised principal component (SuperPC) methods". The TCGA dataset is used as the training cohort, and three CGGA datasets are used as the verification cohorts. We set nodesize as 15, ntree as 1000 and applied Random Seed in machine learning.

The Harrell Consistency Index (C-index) of each model was calculated in the training and verification cohorts. The average C-index of the three independent verification queues is calculated, and the model with the highest average C-index is defined as the most valuable model. The risk score (RS) was established using the RSF algorithm (the same as the most valuable model).

2.5. Survival analysis

Kaplan-Meier (K-M) survival analysis was used to evaluate the prognosis by R package "survival". The survfit function of R software package "survival" was used to analyze the prognostic between different groups. The log-rank test method was used to evaluate the statistical significance [22].

2.6. Operating characteristic curve (ROC) analysis of TNFAIP6

Time-dependent ROC analysis was performed using the "timeROC" R package to display the practice value of TNFAIP6 in predicting 1-, 2-, 3-, 4-, and 5- overall survival (OS). Visualize the data using the 'ggplot 2' R package [23].

2.7. The immune microenvironment of LGG in different TNFAIP6 expression groups

The "ESTIMATE" R package and the single sample gene set enrichment analysis (ssGSEA) were used to calculate the infiltration scores of 28 immune-related cells of each sample [24]. The immune score and stromal score of each sample were also calculated. Wilcoxon rank sum test was used to evaluate the statistical significance between two TNFAIP6 expression group. The association between TNFAIP6 expression and immune checkpoints of each sample was also analyzed.

2.8. Functional analysis

Gene Ontology (GO), Kyoto Encyclopedia of Genes and Genomes (KEGG), Hallmarks and Gene set enrichment analysis (GSEA) were performed using R "clusterProfiler" package [25]. Protein-protein interaction (PPI) analysis was conducted on STRING (https://cn.string-db.org/) and visualized by cytoscape (version 3.7.0).

2.9. Immunohistochemistry

Immunohistochemical (IHC) staining was performed on 18 LGG paraffin sections obtained from 9 LGG samples (3 grade III gliomas and 6 grade II gliomas), which was authorized by the Ethics Committee of Zhujiang Hospital of Southern Medical University. The sections were incubated with primary antibodies against CD133 (rabbit, 1:400; YT5192; Immunoway, America), and TNFAIP6 (rabbit, 1:200; AF5492; Affinity, America). The lHC score was calculated by two experienced pathologists. The samples were divided into two groups according to the median CD133 IHC score.

2.10. Statistical analysis

All statistical analyses were performed using R software (version 4.3.1). The hazard ratio was employed to reflect the effect of genes on prognosis. When HR larger than 1.00, the relative gene is considered as a risk factor. The Wilcoxon rank sum test was used to test the statistical significance between two groups. Correlation analysis was performed using spearman correlation analysis. $P < 0.05$ indicated statistical significance ($p < 0.05$*; $p < 0.01$**; $p < 0.001$***).

3. Results

3.1. Relationship between mDNAsi and the prognosis of LGG patients

The mDNAsi were calculated to evaluate the stem cell levels of each samples and the result suggested that grade III glioma had higher stemness level than grade II glioma, which is consistent with the known fact. Then, all the TCGA samples were grouped into high- and low-stem cell index groups according to the median of mDNAsi score. K-M curve demonstrated that mDNAsi is negatively correlated with the prognosis of LGG patients, that is, patients in high-stem cell index group suffered from significantly poorer prognosis than those in stem cell index group (Fig. 1A and B).

3.2. The identification of GSCRGs by WCGNA

Based on the established gene co-expression network, WCGNA was applied to identified genes that are most correlated with mDNAsi. 14 modules were obtained, and among all the modules, the pink module displayed the closest relationship with mDNAsi (cor $= 0.73$, $p = 1e^{-91}$), which was chose for subsequent analyses. Finally, by setting the GS and MM values (cor. gene MM > 0.8 and cor. gene GS > 0.5), 103 genes were identified as the GSCRGs (Fig. 2A–C).

3.3. Functional enrichment analysis of GSCRGs

GO analysis showed that in cellular components (CC), 103 GSCRGs were mainly enriched in endomembrane system and vesicle (Fig. 3A). In biological processes (BP), the GSCRGs were mainly enriched in processes such as establishment of localization, transportation and cellular response to chemical (Fig. 3B). In molecular function (MF), the GSCRGs were mainly enriched in the activities of signaling receptor binding, enzyme regulator activity and structural molecule activity (Fig. 3C). Hallmark pathway analysis showed that the GCSRGs were mainly concentrated in angiogenesis, apoptosis, cholesterol homeostasis, coagulation and inflammatory

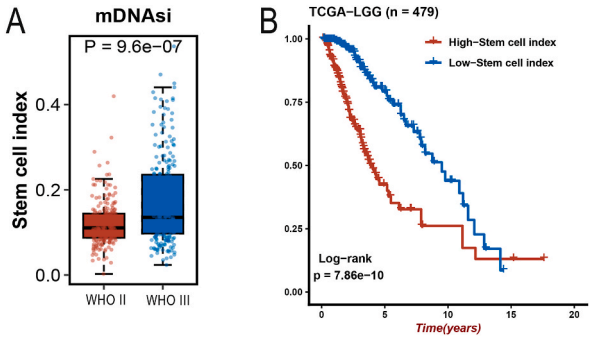

Fig. 1. Survival analysis based on mDNAsi
(A): The mDNAsi level in different grade LGG; (B): Kaplan-Meier curve of OS between high- and low-score groups.

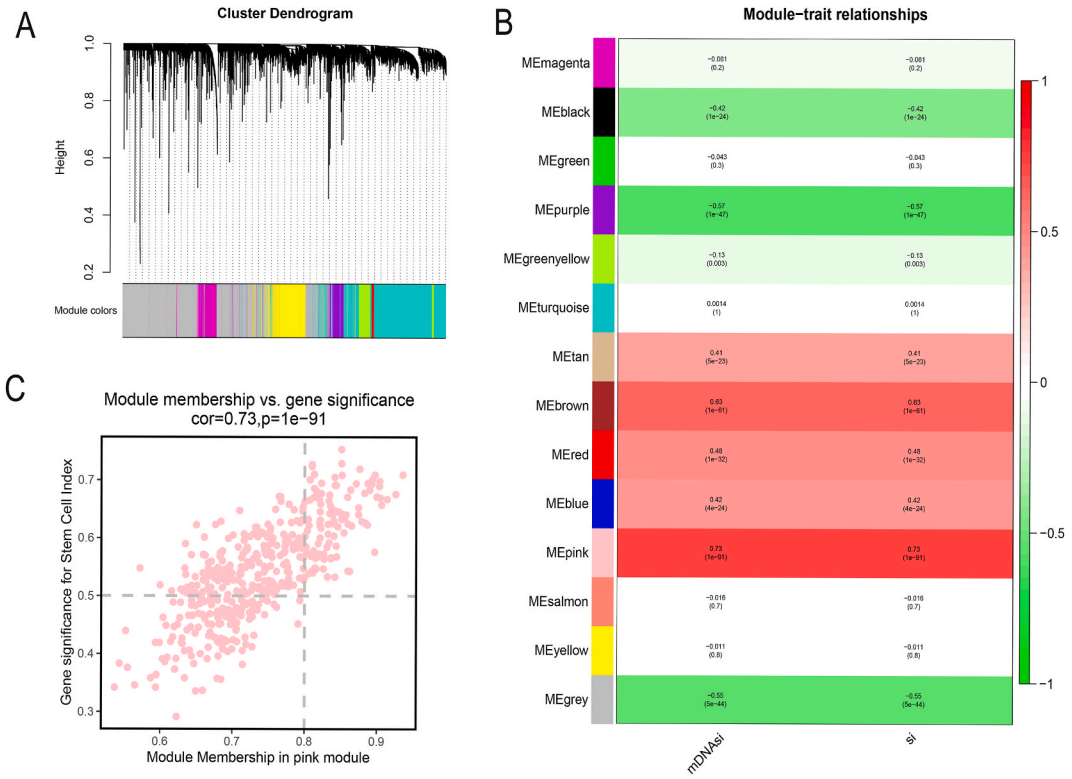

Fig. 2. WCGNA was used to identify genes related to LGG stemness
(A): The cluster dendrogram of WGCNA; (B): The clustered modules of WGCNA; (C): Identification of GSCRGs in the MEpink module.

response pathways (Fig. 3D); while KEGG pathway analysis showed that the GCSRGs were mainly concentrated in hippo signaling pathway, ferroptosis, valine, leucine and isoleucine metabolism, arachidonic acid metabolis and leukocyte transendothelial migration process (Fig. 3E).

3.4. Prognostic GSCRGs signature establishment

The Univariate Cox regression analysis was conducted to pre-screen the potential prognostic GSCRGs, and 95 prognostic GSCRGs were identified (Supplemental Table 1). 10 outstanding machine learning algorithms were conducted, and among 101 different combination models, the model established by RSF algorithm displayed the highest C-index in the TCGA training cohorts. Moreover, only one valuable prognostic GSCRG was identified by RSF algorithms, which is TNFAIP6. The RS of the model was also calculated using the RSF algorithm based on the expression levels of TNFAIP6. Reverse validation presented that TNFAIP6 expression is positively correlated with mDNAsi (Supplemental Fig. 1). K-M curves were conducted in all the cohorts, whose result revealed that high-RS subgroup suffered from significantly poorer prognosis than low-RS subgroup (Fig. 4A–E).

Time-dependent ROC curves were conduct to evaluate the prognostic value of TNFAIP6. Results of ROC curves of 1-, 2-, 3-, 4-, and 5-year OS in TCGA dataset (AUC values, 0.96, 0.97, 0.98, 0.97, 0.97, respectively), CGGA-1 dataset (AUC values, 0.76, 0.81, 0.80, 0.79, 0.75, respectively), CGGA-2 dataset (AUC values, 0.79, 0.82, 0.84, 0.84, 0.84, respectively), and CGGA-3 dataset (AUC values, 0.78, 0.79, 0.78, 0.74, 0.73, respectively). all supported the excellent performance of the TNFAIP6 in evaluating prognosis (Fig. 4F–I).

3.5. TNFAIP6 affects LGG immune microenvironment

Tumor immune microenvironment (TIME) of each LGG sample was evaluated in order to explore the possible reason how TNFAIP6 affect the prognosis. Obviously, the expression level of TNFAIP6 is positively correlated with immune score and stromal score. Strong positive correlations were also observed between TNFAIP6 expression level and classical immune checkpoints, such as PD-L1, PD-1, CTLA4 and so on. Similarly, results also demonstrated that high-RS group suffered from severer immune infiltration. MeTIL analysis also demonstrated that high-RS group suffered from severer infiltration of tumor infiltrating lymphocytes (Fig. 5).

3.6. Functional effects of TNFAIP6 on LGG

GSEA was applied to presented some most differential enriched pathway between two RS groups (Fig. 6A–D). Results demonstrated

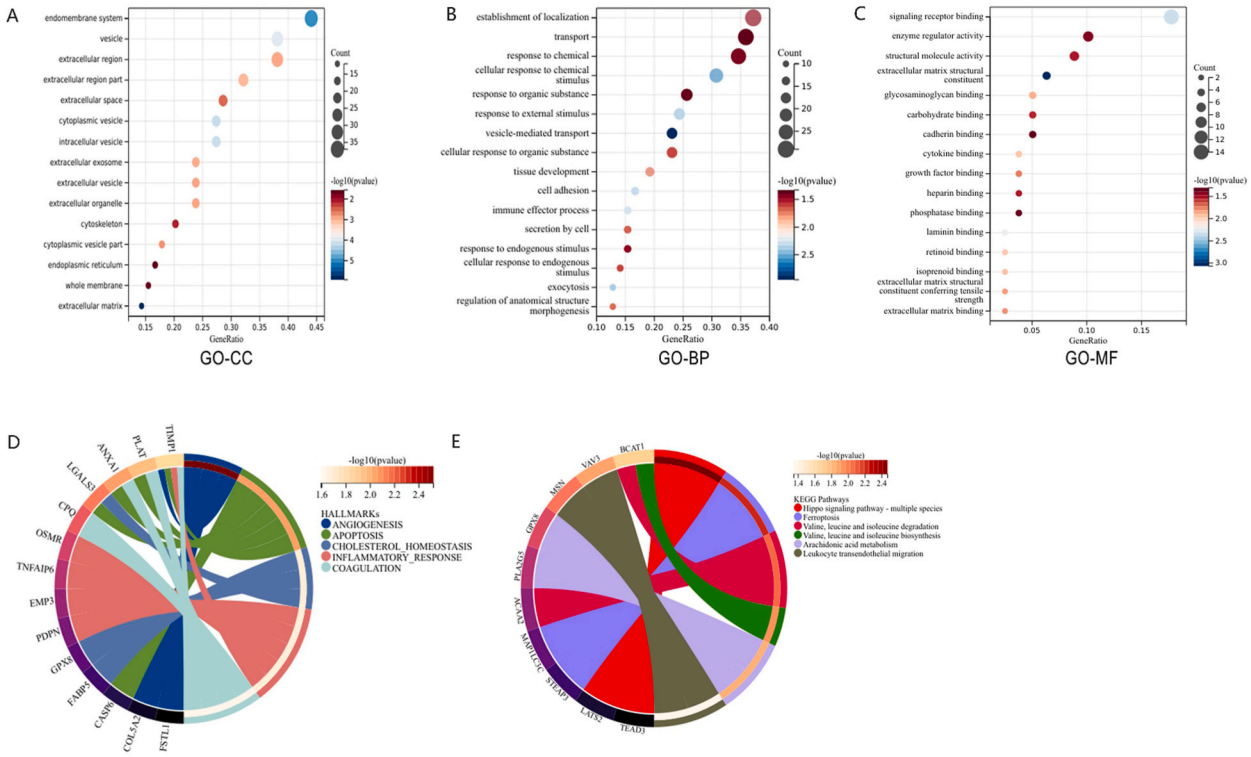

Fig. 3. Functional analysis of 103 GSCRGs
(A): GO analysis in cellular components (CC), biological processes (BP) and molecular function (MF); (B) Hallmark pathway analysis; (C) KEGG pathway analysis.

that intercellular interaction pathways, cell adhesion-related pathways, classic pro-cancer pathways, inflammation signaling pathway and immunology signaling pathway were all enriched in high TNFAIP6 expression group, which indicated that LGG of high TNFAIP6 expression group had more malignant biological behavioral characteristics. PPI network revealed the top 50 proteins that are closely related to TNFAIP6, which included CD44, a novel glioma stem cell marker, and some kinds of inflammatory factors, such as IL-1B and IL-6, and so on (Fig. 6E).

3.7. Expression level of TNFAIP6 in different stemness groups

CD133 is a widely acknowledged GSCs marker, therefore, we divided ther Zhujiang cohort into high- and low-stemness groups based on the expression levels of CD133. According to the median pathology score of CD133, 5 samples were included in the low-stemness group, and 4 samples were classified into high-stemness group. The results displayed that the expression level of TNFAIP6 has strong correlation with CD133 (cor. = 0.74, $p < 0.02$) (Fig. 7A–C).

4. Discussion

LGG accounts for about 43.2 % of gliomas, and the prognosis of patients varies greatly [26,27]. Some patients may experience the same extremely short survival time as glioblastoma patients, while others may luckily achieve clinical cure, which may due to the heterogeneity of the glioma itself [28–30]. Because GSCs have the characteristics of proliferation, differentiation, and drug resistance, they are thought to be the main responsible for the heterogeneity [15,31,32]. Therefore, further exploration of more specific GSC markers and potential therapeutic targets is the priority in current research.

Based on the above description, this study is aiming to explore the potential impact of GSCRGs on the prognosis of LGG patients and to establish a robust prognosis prediction model. We used mDNAsi and WCGNA to identify the GSCRGs, and 10 machine learning algorithms was applied to establish a robust and stable prognosis prediction model. Finally, the result suggested that the model constructed by RSF algorithms is the most valuable one, no matter in training cohort or in validation cohorts. Notably, only TNFAIP6 was included in this high-value prognostic model. Both survival analysis and time-depend ROC analysis display the excellent performance of TNFAIP6 in evaluating prognosis.

TNFAIP6 (aliases: TSG-6) was firstly discovered in 1990 by Lee et al. [33], which was subsequently found to be a secreted protein composed of 260 amino acids [34]. As a kind of secreted protein, TNFAIP6 has been shown to be associated with cell stemness. It can

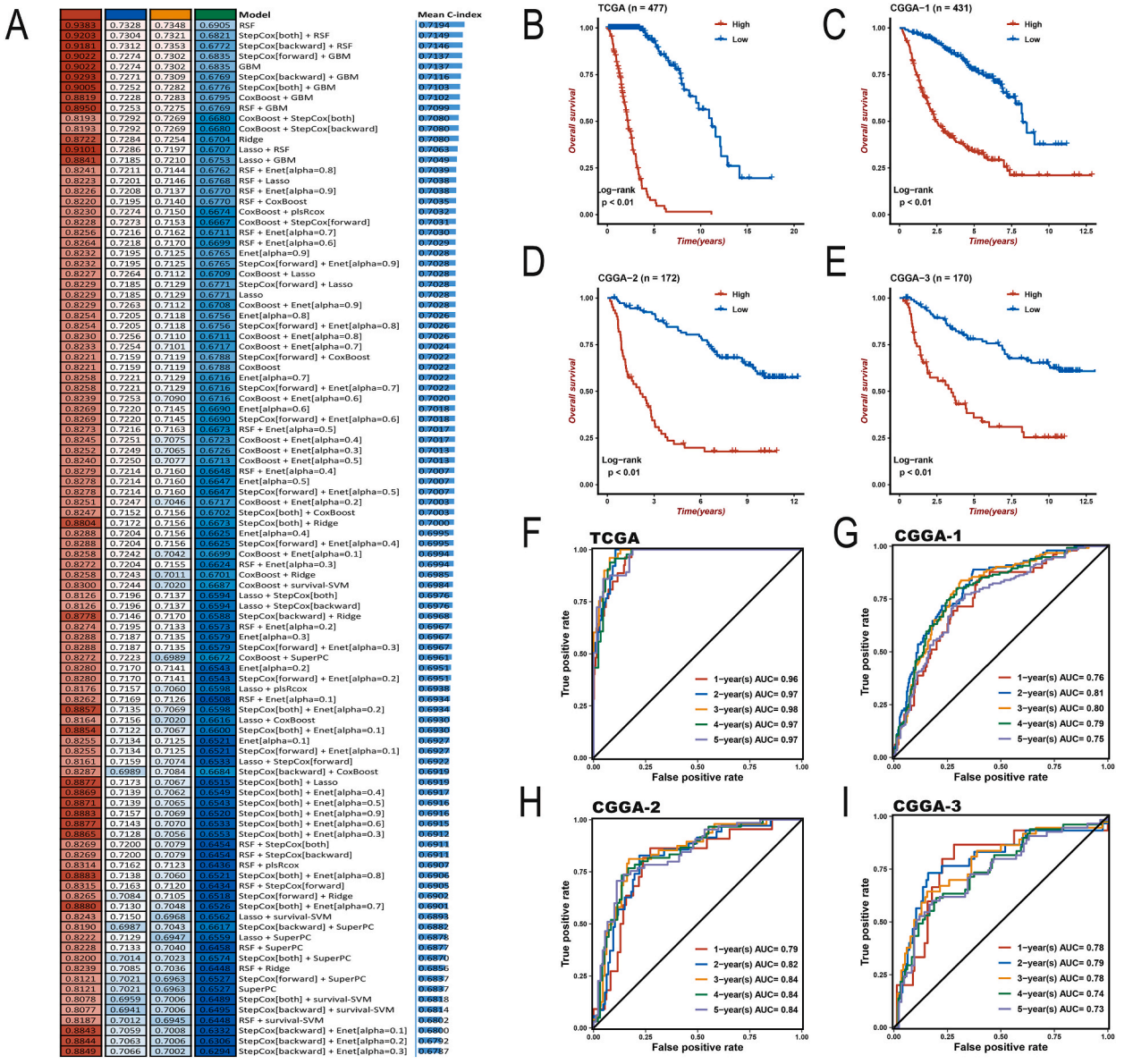

Fig. 4. Establishment of prognostic GSCRG signature

(A): 101 combination models of 10 machine learning algorithms; (B–E): Survival analysis between LGG patients with high and low RS; (F–I): The Time-dependent ROC curves of 1-, 2-, 3-, 4-, and 5-year OS in the training and validation cohorts.

bind to hyaluronic acid (HA) and stabilized CD44 (a novel GSCs marker) by regulate the interaction between HA and CD44 [35], and therefore promoted the formation of CD44-EGFR complex on the cell membrane, which induced ERK activation and epithelial-mesenchymal transition, ultimately leading to the metastasis and invasion of tumor cells [36]. Moreover, TNFAIP6 has been identified as a potential cellular marker of mouse mesenchymal stem cells (MSCs) and its anti-inflammatory and immunosuppression function have been demonstrated in multiple models outside of glioma [37–40].

However, there is still a lack of research on TNFAIP6 in LGG. Our study found that the expression level of TNFAIP6 was significantly positively correlated with immune score, stromal score and classical immune checkpoint expression, which indicated that LGG with high expression of TNFAIP6 suffered from severer immunosuppression. Existing studies have clarified that immune checkpoint molecules play an immunosuppressive role in tumors [41], for instance, the increased expression of PD-1 and its ligand PD-L1 reduced the activity of both $CD8^+$ and $CD4^+$ T lymphocytes, and inhibit their proliferation, thereby contributing to a suppressive immune ircoenvironment in tumor [42–44]; CTLA-4, a classic negative regulator of T cell activation and function, can transduce inhibitory signals by antagonizing the activity of co-stimulatory ligands on CD28 [45–47]. Similarly, higher immune cell infiltration abundance is also associated with immunosuppression [48–51]. Current research believed that the increased infiltration of immune cells in glioma

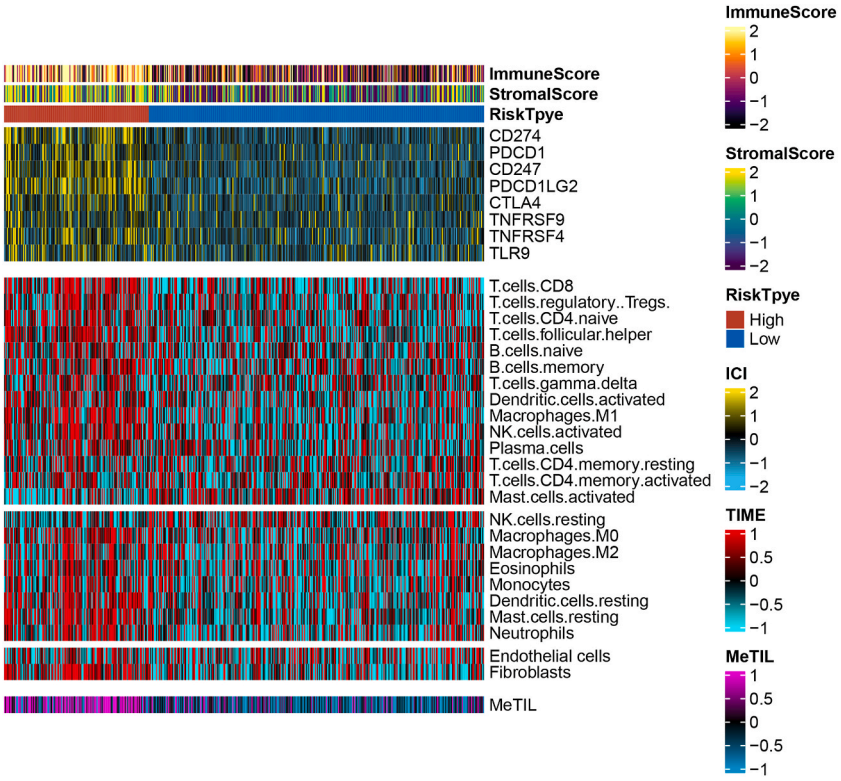

Fig. 5. Immune-related characteristics of different RS group
Heatmap revealing the correlation between different RS group and immune-related characteristics.

burdened the anti-glioma immune and resulted in the formation of immunosuppressive microenvironment [52–54]. Moreover, a study on lung adenocarcinoma directly revealed that TNFAIP6 led to 'N2' subtype neutrophil polarization, thereby promoting lung adenocarcinoma development [55]. Based on the above statement, we inferred that the high expression of TNFAIP6 may affect the prognosis by enhancing the stemness of LGG cells and strengthening immunosuppression.

Function analysis further verified the above result. It is obviously to see that various immune cells signaling pathways and inflammatory signaling pathways were enriched in TNFAIP6 high expression group, while pro-cancer pathways also significantly enriched in high TNFAIP6 expression group, especially p53 pathway and glioma pathway. These suggested that TNFAIP6 high expression LGG had more malignant biological behaviors. Besides, the result of immunohistochemistry further verified that TNFAIP6 is highly glioma stemness related.

5. Conclusion

Our study established a robust and stable LGG prognosis prediction model by conduct a series of bioinformatics analysis. Finally, TNFAIP6 was identified as the most valuable prognostic GSCRG, and the classification based on theexpression of TNFAIP6 can accurately reflect the biological characteristics of different LGG samples. Moreover, as we know, our study innovative focus on the impact of TNFAIP6 on LGG, making up for the vacancy of previous research and provides a new research direction. In all, TNFAIP6 may be a novel marker of glioma stem cells, playing an essential role in the regulation of LGG microenvironment and prognosis prediction.

Ethics approval and consent to participate

The acquisition of samples was approved by the Ethics Committee of Zhujiang Hospital of Southern Medical University. Ethical approval number：2023-KY-327-01.

Consent for publication

All authors have read and approved the manuscript.

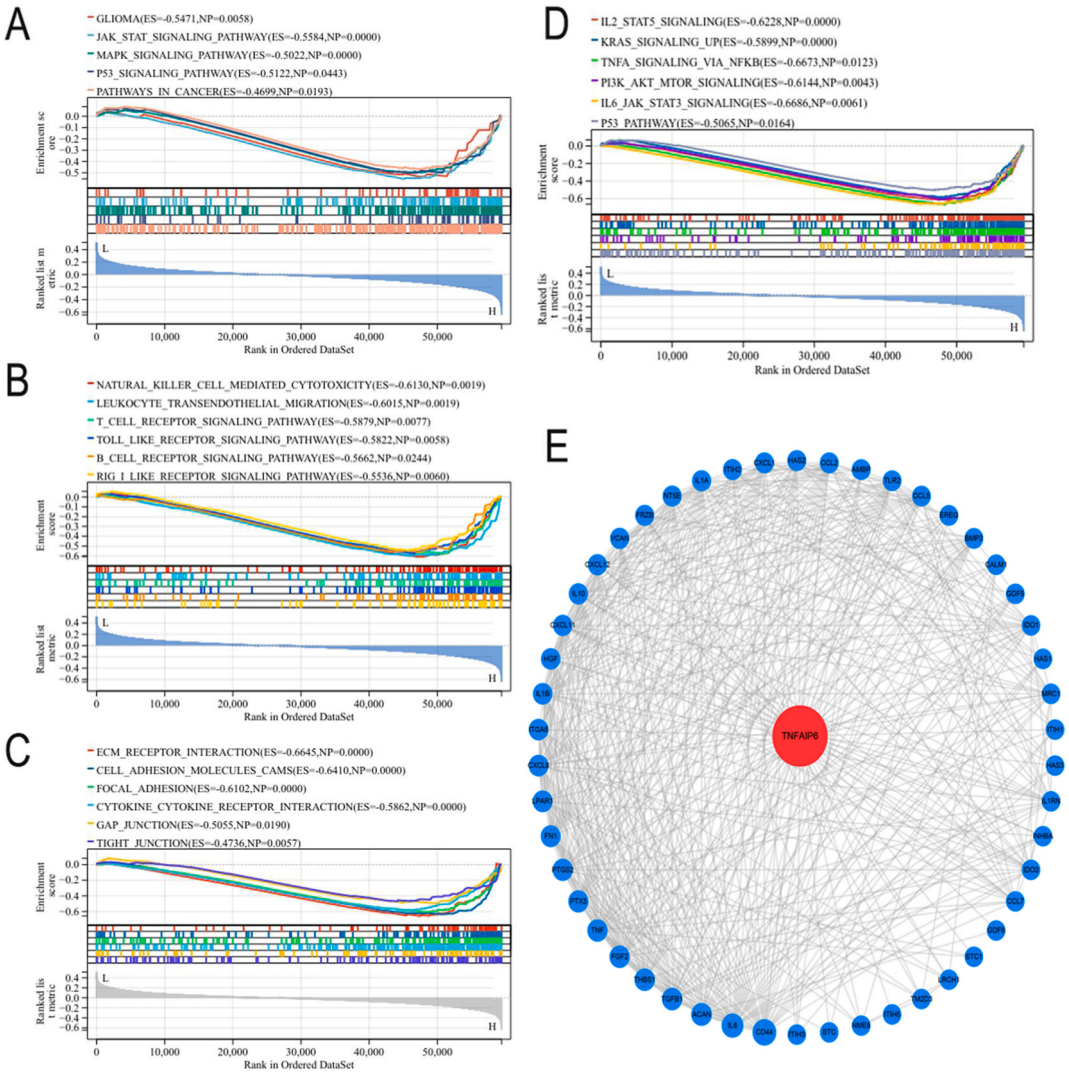

Fig. 6. Functional analysis between two TNFAIP6 expression group
(A-C): GSEA analysis based on KEGG dataset to explore the differences between two TNFAIP6 expression group; (D): GSEA analysis based on Hallmark dataset to verify the KEGG result; (E): The PPI diagram showed top 50 proteins that were closely related to TNFAIP6. The larger the node is, the closer relationship it has to TNFAIP6.

Competing interests

The author reports no conflicts of interest in this work.

Funding

Yiquan Ke received funding from the National Natural Science Foundation of China (No. 82072762); Jihui Wang received funding from the China Postdoctoral Science Foundation (No. 2020M672737) and the President Foundation of ZhuJiang Hospital, Southern Medical University (No. yzjj2018rc04).

Availability of data and materials

The DNA methylation data, RNA sequencing data and corresponding clinical information of glioma patients were derived from the Cancer Genome Atlas (TCGA, https://portal.gdc.cancer.gov); Chinese Glioma Genome Atlas (CGGA, http://www.cgga.org.cn/). Specifically, 477 LGG samples from TCGA; 431 LGG samples (CGGA-1) from CGGA mRNAseq-693 dataset, 172 LGG samples (CGGA-2) from CGGA mRNAseq-325 dataset, 170 LGG samples (CGGA-3) from CGGA mRNA-array-301 dataset. The original code and any

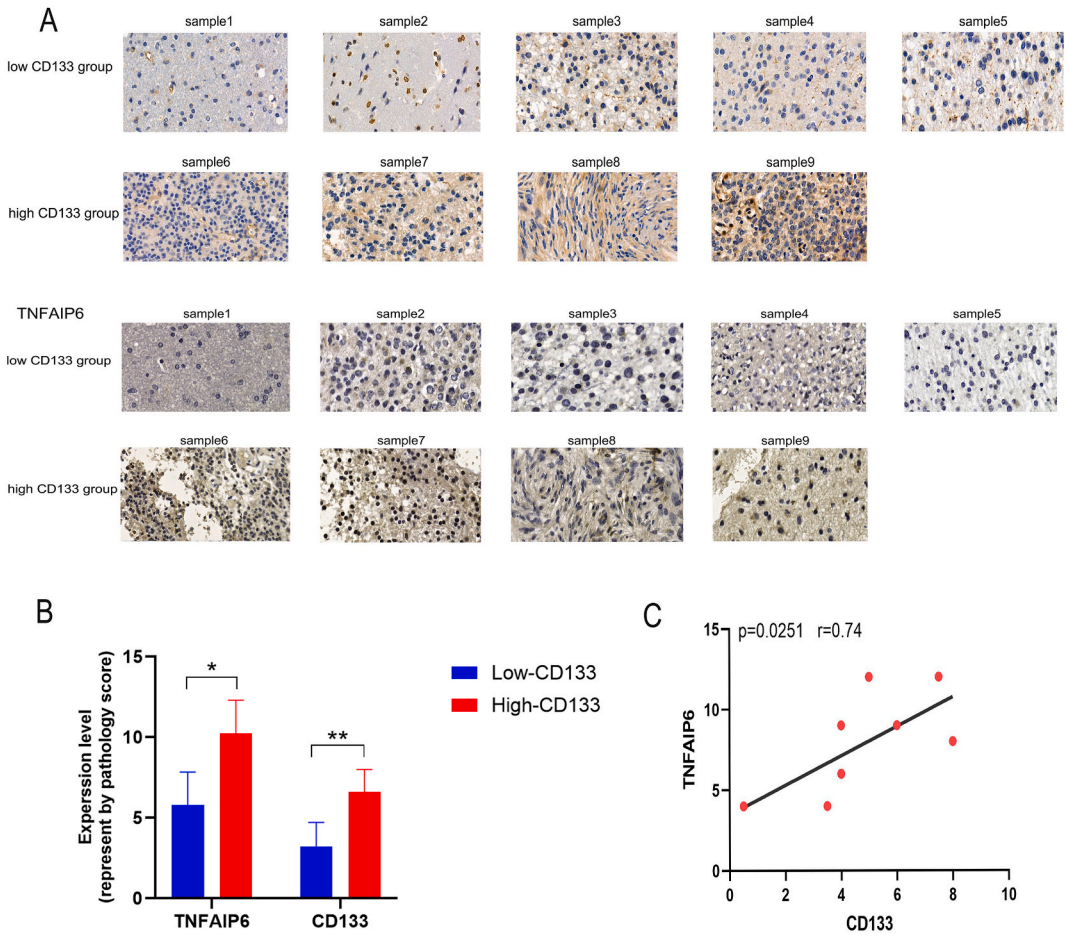

Fig. 7. Expression level of TNFAIP6 in Low- and High- CD133 expression groups
(A): Representative IHC staining images of CD133 and TNFAIP6 in two stemness group in the Zhujiang in-house cohort. (B): Box plot displaying the pathology score levels of TNFAIP6 and CD133 based between two stemness group in the Zhujiang in-house dataset; (C): The correlation of expression level between TNFAIP6 and CD133.

additional information required to reanalyze the data reported in this paper is available from the lead contact upon request.

CRediT authorship contribution statement

Qinhong Huang: Writing – original draft, Methodology, Data curation, Conceptualization. **Hui Liang:** Writing – original draft, Software. **Shenbao Shi:** Writing – original draft, Methodology, Formal analysis, Data curation. **Yiquan Ke:** Writing – review & editing, Project administration, Funding acquisition. **Jihui Wang:** Writing – review & editing, Project administration, Funding acquisition.

Declaration of competing interest

The authors declare the following financial interests/personal relationships which may be considered as potential competing interests: Yiquan Ke reports a relationship with National Natural Science Foundation of China that includes: funding grants. Jihui Wang reports a relationship with China Postdoctoral Science Foundation that includes: funding grants. Jihui Wang reports a relationship with President Foundation of ZhuJiang Hospital, Southern Medical University that includes: funding grants. If there are other authors, they declare that they have no known competing financial interests or personal relationships that could have appeared to influence the work reported in this paper.

Appendix A. Supplementary data

Supplementary data to this article can be found online at https://doi.org/10.1016/j.heliyon.2024.e33030.

References

[1] D.N. Louis, A. Perry, P. Wesseling, D.J. Brat, I.A. Cree, D. Figarella-Branger, C. Hawkins, H.K. Ng, S.M. Pfister, G. Reifenberger, et al., The 2021 WHO classification of tumors of the central nervous system: a summary, Neuro Oncol. 23 (8) (2021) 1231–1251.
[2] P. Śledzińska, M.G. Bebyn, J. Furtak, J. Kowalewski, M.A. Lewandowska, Prognostic and predictive biomarkers in gliomas, Int. J. Mol. Sci. 22 (19) (2021).
[3] L. Capelle, D. Fontaine, E. Mandonnet, L. Taillandier, J.L. Golmard, L. Bauchet, J. Pallud, P. Peruzzi, M.H. Baron, M. Kujas, et al., Spontaneous and therapeutic prognostic factors in adult hemispheric World Health Organization Grade II gliomas: a series of 1097 cases: clinical article, J. Neurosurg. 118 (6) (2013) 1157–1168.
[4] D.J. Brat, R.G. Verhaak, K.D. Aldape, W.K. Yung, S.R. Salama, L.A. Cooper, E. Rheinbay, C.R. Miller, M. Vitucci, O. Morozova, et al., Comprehensive, integrative genomic analysis of diffuse lower-grade gliomas, N. Engl. J. Med. 372 (26) (2015) 2481–2498.
[5] T. Jiang, Y. Mao, W. Ma, Q. Mao, Y. You, X. Yang, C. Jiang, C. Kang, X. Li, L. Chen, et al., CGCG clinical practice guidelines for the management of adult diffuse gliomas, Cancer Lett. 375 (2) (2016) 263–273.
[6] G. Li, F. Wu, F. Zeng, Y. Zhai, Y. Feng, Y. Chang, D. Wang, T. Jiang, W. Zhang, A novel DNA repair-related nomogram predicts survival in low-grade gliomas, CNS Neurosci. Ther. 27 (2) (2021) 186–195.
[7] A. Pace, L. Dirven, J.A.F. Koekkoek, H. Golla, J. Fleming, R. Rudà, C. Marosi, E. Le Rhun, R. Grant, K. Oliver, et al., European Association for Neuro-Oncology (EANO) guidelines for palliative care in adults with glioma, Lancet Oncol. 18 (6) (2017) e330–e340.
[8] A.C. Tan, D.M. Ashley, G.Y. López, M. Malinzak, H.S. Friedman, M. Khasraw, Management of glioblastoma: state of the art and future directions, Ca - Cancer J. Clin. 70 (4) (2020) 299–312.
[9] M. Mijiti, A. Maimaiti, X. Chen, M. Tuersun, M. Dilixiati, Y. Dilixiati, G. Zhu, H. Wu, Y. Li, M. Turhon, et al., CRISPR-cas9 screening identified lethal genes enriched in Hippo kinase pathway and of predictive significance in primary low-grade glioma, Mol. Med. 29 (1) (2023) 64.
[10] L. Yang, P. Shi, G. Zhao, J. Xu, W. Peng, J. Zhang, G. Zhang, X. Wang, Z. Dong, F. Chen, et al., Targeting cancer stem cell pathways for cancer therapy, Signal Transduct. Targeted Ther. 5 (1) (2020) 8.
[11] T. Huang, X. Song, D. Xu, D. Tiek, A. Goenka, B. Wu, N. Sastry, B. Hu, S.Y. Cheng, Stem cell programs in cancer initiation, progression, and therapy resistance, Theranostics 10 (19) (2020) 8721–8743.
[12] R. Paul, J.F. Dorsey, Y. Fan, Cell plasticity, senescence, and quiescence in cancer stem cells: biological and therapeutic implications, Pharmacol. Ther. 231 (2022) 107985.
[13] L. Vermeulen, F. de Sousa e Melo, D.J. Richel, J.P. Medema, The developing cancer stem-cell model: clinical challenges and opportunities, Lancet Oncol. 13 (2) (2012) e83–e89.
[14] J.P. Medema, Cancer stem cells: the challenges ahead, Nat. Cell Biol. 15 (4) (2013) 338–344.
[15] M.L. Suvà, I. Tirosh, The glioma stem cell model in the era of single-cell genomics, Cancer Cell 37 (5) (2020) 630–636.
[16] G. Ferrandina, M. Petrillo, G. Bonanno, G. Scambia, Targeting CD133 antigen in cancer, Expert Opin. Ther. Targets 13 (7) (2009) 823–837.
[17] K. Biserova, A. Jakovlevs, R. Uljanovs, I. Strumfa, Cancer stem cells: significance in origin, pathogenesis and treatment of glioblastoma, Cells 10 (3) (2021).
[18] S. Bao, Q. Wu, R.E. McLendon, Y. Hao, Q. Shi, A.B. Hjelmeland, M.W. Dewhirst, D.D. Bigner, J.N. Rich, Glioma stem cells promote radioresistance by preferential activation of the DNA damage response, Nature 444 (7120) (2006) 756–760.
[19] Y. Wei, Q. Chen, S. Huang, Y. Liu, Y. Li, Y. Xing, D. Shi, W. Xu, W. Liu, Z. Ji, et al., The interaction between DNMT1 and high-mannose CD133 maintains the slow-cycling state and tumorigenic potential of glioma stem cell, Adv. Sci. 9 (26) (2022) e2202216.
[20] T.M. Malta, A. Sokolov, A.J. Gentles, T. Burzykowski, L. Poisson, J.N. Weinstein, B. Kamińska, J. Huelsken, L. Omberg, O. Gevaert, et al., Machine learning identifies stemness features associated with oncogenic dedifferentiation, Cell 173 (2) (2018) 338–354.e315.
[21] S. Morabito, E. Miyoshi, N. Michael, S. Shahin, A.C. Martini, E. Head, J. Silva, K. Leavy, M. Perez-Rosendahl, V. Swarup, Single-nucleus chromatin accessibility and transcriptomic characterization of Alzheimer's disease, Nat. Genet. 53 (8) (2021) 1143–1155.
[22] T.G. Clark, M.J. Bradburn, S.B. Love, D.G. Altman, Survival analysis part I: basic concepts and first analyses, Br. J. Cancer 89 (2) (2003) 232–238.
[23] J.V. Carter, J. Pan, S.N. Rai, S. Galandiuk, ROC-ing along: evaluation and interpretation of receiver operating characteristic curves, Surgery 159 (6) (2016) 1638–1645.
[24] Y. Chen, Y. Feng, F. Yan, Y. Zhao, H. Zhao, Y. Guo, A novel immune-related gene signature to identify the tumor microenvironment and prognose disease among patients with oral squamous cell carcinoma patients using ssGSEA: a bioinformatics and biological validation study, Front. Immunol. 13 (2022) 922195.
[25] A. Subramanian, P. Tamayo, V.K. Mootha, S. Mukherjee, B.L. Ebert, M.A. Gillette, A. Paulovich, S.L. Pomeroy, T.R. Golub, E.S. Lander, et al., Gene set enrichment analysis: a knowledge-based approach for interpreting genome-wide expression profiles, Proc. Natl. Acad. Sci. U. S. A. 102 (43) (2005) 15545–15550.
[26] H. Suzuki, K. Aoki, K. Chiba, Y. Sato, Y. Shiozawa, Y. Shiraishi, T. Shimamura, A. Niida, K. Motomura, F. Ohka, et al., Mutational landscape and clonal architecture in grade II and III gliomas, Nat. Genet. 47 (5) (2015) 458–468.
[27] T. Jiang, D.H. Nam, Z. Ram, W.S. Poon, J. Wang, D. Boldbaatar, Y. Mao, W. Ma, Q. Mao, Y. You, et al., Clinical practice guidelines for the management of adult diffuse gliomas, Cancer Lett. 499 (2021) 60–72.
[28] A. Ou, W.K.A. Yung, N. Majd, Molecular mechanisms of treatment resistance in glioblastoma, Int. J. Mol. Sci. 22 (1) (2020).
[29] J.G. Nicholson, H.A. Fine, Diffuse glioma heterogeneity and its therapeutic implications, Cancer Discov. 11 (3) (2021) 575–590.
[30] M.W. Yu, D.F. Quail, Immunotherapy for glioblastoma: current progress and challenges, Front. Immunol. 12 (2021) 676301.
[31] E. Lee, R.L. Yong, P. Paddison, J. Zhu, Comparison of glioblastoma (GBM) molecular classification methods, Semin. Cancer Biol. 53 (2018) 201–211.
[32] K. Zhou, Y.L. Yao, Z.C. He, C. Chen, X.N. Zhang, K.D. Yang, Y.Q. Liu, Q. Liu, W.J. Fu, Y.P. Chen, et al., VDAC2 interacts with PFKP to regulate glucose metabolism and phenotypic reprogramming of glioma stem cells, Cell Death Dis. 9 (10) (2018) 988.
[33] T.H. Lee, G.W. Lee, E.B. Ziff, J. Vilcek, Isolation and characterization of eight tumor necrosis factor-induced gene sequences from human fibroblasts, Mol. Cell Biol. 10 (5) (1990) 1982–1988.
[34] T.H. Lee, H.G. Wisniewski, J. Vilcek, A novel secretory tumor necrosis factor-inducible protein (TSG-6) is a member of the family of hyaluronate binding proteins, closely related to the adhesion receptor CD44, J. Cell Biol. 116 (2) (1992) 545–557.
[35] A.J. Day, C.M. Milner, TSG-6: a multifunctional protein with anti-inflammatory and tissue-protective properties, Matrix Biol. 78–79 (2019) 60–83.
[36] B. Liu, T. Liu, Y. Liu, X. Feng, X. Jiang, J. Long, S. Ye, D. Chen, J. Wang, Z. Yang, TSG-6 promotes cancer cell aggressiveness in a CD44-dependent manner and reprograms normal fibroblasts to create a pro-metastatic microenvironment in colorectal cancer, Int. J. Biol. Sci. 18 (4) (2022) 1677–1694.
[37] R.H. Lee, A.A. Pulin, M.J. Seo, D.J. Kota, J. Ylostalo, B.L. Larson, L. Semprun-Prieto, P. Delafontaine, D.J. Prockop, Intravenous hMSCs improve myocardial infarction in mice because cells embolized in lung are activated to secrete the anti-inflammatory protein TSG-6, Cell Stem Cell 5 (1) (2009) 54–63.
[38] R. Li, W. Liu, J. Yin, Y. Chen, S. Guo, H. Fan, X. Li, X. Zhang, X. He, C. Duan, TSG-6 attenuates inflammation-induced brain injury via modulation of microglial polarization in SAH rats through the SOCS3/STAT3 pathway, J. Neuroinflammation 15 (1) (2018) 231.
[39] Y. Jiang, L.M. Glasstetter, A. Lerman, L.O. Lerman, TSG-6 (tumor necrosis factor-α-stimulated gene/protein-6): an emerging remedy for renal inflammation, Hypertension 80 (1) (2023) 35–42.
[40] L. Li, L. Yang, X. Chen, X. Chen, L. Diao, Y. Zeng, J. Xu, TNFAIP6 defines the MSC subpopulation with enhanced immune suppression activities, Stem Cell Res. Ther. 13 (1) (2022) 479.
[41] J.A. Marin-Acevedo, E.O. Kimbrough, Y. Lou, Next generation of immune checkpoint inhibitors and beyond, J. Hematol. Oncol. 14 (1) (2021) 45.
[42] D. Daassi, K.M. Mahoney, G.J. Freeman, The importance of exosomal PDL1 in tumour immune evasion, Nat. Rev. Immunol. 20 (4) (2020) 209–215.
[43] S. Spranger, R. Bao, T.F. Gajewski, Melanoma-intrinsic β-catenin signalling prevents anti-tumour immunity, Nature 523 (7559) (2015) 231–235.
[44] X. Guo, Y. Zhang, L. Zheng, C. Zheng, J. Song, Q. Zhang, B. Kang, Z. Liu, L. Jin, R. Xing, et al., Global characterization of T cells in non-small-cell lung cancer by single-cell sequencing, Nat. Med. 24 (7) (2018) 978–985.
[45] S.L. Topalian, C.G. Drake, D.M. Pardoll, Immune checkpoint blockade: a common denominator approach to cancer therapy, Cancer Cell 27 (4) (2015) 450–461.

[46] B. Rowshanravan, N. Halliday, D.M. Sansom, CTLA-4: a moving target in immunotherapy, Blood 131 (1) (2018) 58–67.
[47] S.C. Wei, C.R. Duffy, J.P. Allison, Fundamental mechanisms of immune checkpoint blockade therapy, Cancer Discov. 8 (9) (2018) 1069–1086.
[48] R.D. Schreiber, L.J. Old, M.J. Smyth, Cancer immunoediting: integrating immunity's roles in cancer suppression and promotion, Science 331 (6024) (2011) 1565–1570.
[49] J. Peng, B.F. Sun, C.Y. Chen, J.Y. Zhou, Y.S. Chen, H. Chen, L. Liu, D. Huang, J. Jiang, G.S. Cui, et al., Single-cell RNA-seq highlights intra-tumoral heterogeneity and malignant progression in pancreatic ductal adenocarcinoma, Cell Res. 29 (9) (2019) 725–738.
[50] L. Zhang, Z. Li, K.M. Skrzypczynska, Q. Fang, W. Zhang, S.A. O'Brien, Y. He, L. Wang, Q. Zhang, A. Kim, et al., Single-cell analyses inform mechanisms of myeloid-targeted therapies in colon cancer, Cell 181 (2) (2020) 442–459.e429.
[51] K.C. Kao, S. Vilbois, C.H. Tsai, P.C. Ho, Metabolic communication in the tumour-immune microenvironment, Nat. Cell Biol. 24 (11) (2022) 1574–1583.
[52] L. Barthel, M. Hadamitzky, P. Dammann, M. Schedlowski, U. Sure, B.K. Thakur, S. Hetze, Glioma: molecular signature and crossroads with tumor microenvironment, Cancer Metastasis Rev. 41 (1) (2022) 53–75.
[53] C. Lin, N. Wang, C. Xu, Glioma-associated microglia/macrophages (GAMs) in glioblastoma: immune function in the tumor microenvironment and implications for immunotherapy, Front. Immunol. 14 (2023) 1123853.
[54] M.A. Jayaram, J.J. Phillips, Role of the microenvironment in glioma pathogenesis, Annu. Rev. Pathol. 19 (2024) 181–201.
[55] R. Liu, G. Zhu, Y. Sun, M. Li, Z. Hu, P. Cao, X. Li, Z. Song, J. Chen, Neutrophil infiltration associated genes on the prognosis and tumor immune microenvironment of lung adenocarcinoma, Front. Immunol. 14 (2023) 1304529.